Mini Review

Check for updates

Molecular engineering toward large pore-sized covalent organic frameworks

Xiao Li[1,2], Keyu Geng[3], Shuai Fu[4], Enquan Jin[1,2,*] (iD)

[1]State Key Laboratory of Inorganic Synthesis and Preparative Chemistry, College of Chemistry, Jilin University, Changchun 130012, Jilin, China.
[2]International Center of Future Science, Jilin University, Changchun 130012, Jilin, China.
[3]Procter & Gamble Technology (Beijing) Co., Ltd, Beijing 101312, China.
[4]Center for Advancing Electronics Dresden (cfaed) and Faculty of Chemistry and Food Chemistry, Technische Universität Dresden, Dresden 01062, Germany.

[*]**Correspondence to:** Prof. Enquan Jin, State Key Laboratory of Inorganic Synthesis and Preparative Chemistry, College of Chemistry, Jilin University, 2699 Qianjin Street, Changchun 130012, Jilin, China. E-mail: enquanjin@jlu.edu.cn

How to cite this article: Li X, Geng K, Fu S, Jin E. Molecular engineering toward large pore-sized covalent organic frameworks. *Chem Synth* 2024;4:15. https://dx.doi.org/10.20517/cs.2023.63

Abstract

In recent years, covalent organic frameworks (COFs) as designable crystalline porous polymers have attracted widespread attention because of their tunable structures and functionalities. In particular, the unique characteristics of COFs, such as readily controllable pore size, high surface area, editable pore surface environment, and exceptional chemical stability, provide a structural basis for loading large-sized organic, inorganic, and biological molecules for hetero-catalysis, energy storage, and other applications. In this review, we discuss state-of-the-art strategies for the structural design and synthesis, properties, and functionalities of large pore size two-dimensional and three-dimensional COFs, spotlighting recent breakthrough achievements and remarkable progress to guide further efforts in this field.

Keywords: Large pore size, covalent organic frameworks, mesopore, macromolecule absorption

INTRODUCTION

Exploring crystalline porous materials has recently become a focal research topic due to their great potential in solving energy and environmental issues and promoting sustainable social development[1-3]. Covalent

organic frameworks (COFs) integrate organic building blocks into an ordered lattice through covalent bonds. With the advantages of their ordered and stable pore structure, large specific surface area, and functionalizable skeleton, COFs have elicited growing interest and have been widely applied in numerous fields[4], such as gas separation and sorption, catalysis, energy storage and conversion, sensors, semiconductors, spintronics, drug delivery, water desalination, *etc.* Since the first synthesis of boronic ester-linked COF by Côté *et al.* in 2005[5], in 2007, their group reported four examples of three-dimensional (3D) COFs, namely COF-102, COF-103, COF-105, and COF-108[6]. In 2016, Zhuang *et al.* reported for the first carbon-carbon double-bond connected stable COF, two-dimensional (2D) poly(phenelyenevinylene) framework (2DPPV), which has an attractive application prospect in the field of optoelectronics due to the high degree of π-π conjugation[7]. In 2017, Jin *et al.* also reported a similar carbon-carbon double-bond connected COF, sp²c-COF, with full sp²c conjugation covering the fundamental properties of COFs in terms of magnetism, free radicals, and so on[8]. In the same year, Ma *et al.* achieved the first large-size, single-crystal growth and X-ray diffraction (SXRD) structure analysis of 3D COFs based on imine bonding[9]. Over the past few decades, hundreds of COFs with versatile chemical and topological structures have been developed[10-18]. The representative advantages of COFs over other porous analogs, such as zeolites, metal-organic frameworks (MOFs), polymers of intrinsic microporosity (PIMs), covalent triazine frameworks (CTFs), *etc.,* lie in the larger pore size, stable and ordered nature, exceptionally high surface area, and controllable functionalization by pore-surface engineering.

To date, most reported COFs are micro- or small mesoporous COFs with pore sizes ranging from 0.5 to 4.0 nm. In sharp contrast, COFs with pore sizes larger than 4.0 nm have rarely been reported[19-24] due to difficulty in synthesis and lack of reliable approaches to retain large pore apertures. COFs with larger pores enable the loading, separation, and transfer of larger guest molecules[25-27]. Large pore apertures ensure rapid mass transport in hetero-catalysts. For instance, Zhao *et al.* developed macro-TpBpy-Co with both micro- and macropores, achieving a high oxygen evolution reaction (OER) activity with an overpotential of 380 mV at 10 mA/cm² superior to the microporous COF[28]. For better discussion, we defined pore sizes larger than 4.0 nm in COFs as large pores[29], in contrast to mostly reported micro or small mesoporous COFs. In this sense, the development of COFs with regular networks that can accommodate macromolecules such as proteins or peptides holds great promise for drug delivery and heterogeneous catalysis by providing sufficient diffusion of substrates and products. To this end, recent efforts have been made to explore synthetic routes for large pore-sized COFs, which are expected to significantly expand the scope of practical applications and improve overall performance. Notably, there are versatile synthesis methods of COFs, such as template-assisted[28,30], morphology-controlled[31], mechanochemical, solvothermal synthesis, ionothermal, microwave-assisted, sonochemical[32], *etc.* In light of the superiority of bottom-up synthesis in developing atomically precise structures, we mainly focus on the works of controlling the pore sizes of COFs through hydrothermal synthesis.

OVERVIEW OF 2D COFS WITH LARGE PORES

For the skeleton of 2D COFs, organic motifs undergo topological polymerization via condensation to form layered structures, which are further vertically stacked to form periodic columns through interlayer π-π interactions. The pore size and shape of the formed ordered open nano-channels are closely related to the stacking modules of the 2D layers. Conventional strategies to explore large linkers with intense stacking interactions and suitable solubility have enabled the construction of 2D COFs with well-defined porous structures and pore sizes up to 4.0 nm. However, preparing 2D COFs with even larger pore sizes remains challenging. A key fact hindering the development of COFs with larger pores is that the 2D layers tend to stabilize the networks by lateral sliding, a common way of reducing free energy in COFs. In 2010, based on the Density Functional Theory (DFT), Lukose *et al.* proposed four interlayer stacking modes of 2D COFs,

namely, eclipsed (AA), staggered (AB), serrated, and inclined stacking[33,34]. According to this work, 2D COFs tend to stack in a way that exhibits the lowest energy. AA stacking is most likely to construct large pores due to enough space for alleviating steric repulsion, while AB or ABC stacking is difficult to construct large pores due to significant interlayer slipping. Consequently, the pore size and surface area of COFs are diminished because of the structural collapse and pore occlusion, which limits the successful construction of large pore-sized structures.

To date, several promising approaches have been developed to address this crucial issue. They can generally be classified as follows: (A) rational design of 2D COFs with honeycomb (hcb) and kagome (kgm) topologies, which make it easier to form larger pore size compared to other topologies; (B) employing specific linkages such as imides to generate large mesopores in the skeleton of 2D COFs; (C) using large molecule-sized building blocks with charged parts or branched side-chains to prevent the pore shrinkage and interlayer slippage, resulting in the formation of 2D COFs with large pores.

Topology-oriented synthetic strategy

Along with the report of Star-COF-1, Star-COF-2, and Star-COF-3 with pore sizes of 3.9, 4.6, and 4.7 nm by Feng *et al.* in 2012, the kgm topological COFs with large pores gradually came into view[35]. In contrast to the dual-pore COF[36] with a pore size of 2.7 nm, synthesized by the condensation of 4,4′,4″,4‴-(ethene-1,1,2,2-tetrayl)-tetraaniline (ETTA) and terephthalaldehyde, the large cyclic fragments of Star-COFs yield larger pore apertures in the center of topology.

In 2016, Crowe *et al.* reported three novel COFs containing homogeneous and heterogeneous distributions of π-conjugated dehydrobenzoannulene (DBA), DBA-12, and DBA-18 units with varied triangular molecular sizes[37]. Polycondensation between the C_3-symmetric monomeric catechol DBA-12 or DBA-18 and C_2-symmetric pyrene-2,7-dibronic acid (PDBA) yielded three kgm topological COFs, 3.8 nm for Py-DBA-COF 1, 4.3 nm for Py-DBA-COF 2, and 4.1 nm for Py-MV-DBA-COF [Figure 1], respectively. The unique kgm lattice composed of large triangular planar molecules enables the formation of large hexagonal pores in the 2D COFs. It is worth noting that the as-synthesized Py-DBA-COF 2 shows excellent luminescent properties and has the largest pore size among solid-state luminescent 2D COFs, which has great potential in the field of optoelectronic applications.

The polycondensations between two C_2-symmetric units or a C_3-symmetric cyclic molecule and a C_2-symmetric unit can produce kgm topotactic COFs [Scheme 1]. Both synthetic routes enable the construction of large pores, demonstrating the superiority of kgm topology in preventing structural collapse. According to the comparison, the C_3-symmetric cyclic unit-based COFs exhibit larger pores, which could be a promising platform for extending structural diversity.

Linkage-oriented synthetic strategy

COFs can be attached through a variety of methods, such as the boronate esters, triazines, azine bonds, *β*-ketoenamines, *etc.* In 2015, Jin *et al.* reported a series of donor-acceptor COFs named D_{CuPc}-A_{PyrDI}-COF, D_{NiPc}-A_{PyrDI}-COF, D_{CuPc}-A_{NDI}-COF, D_{NiPc}-A_{NDI}-COF, D_{CuPc}-A_{PDI}-COF, and D_{ZnPc}-A_{PDI}-COF with pore sizes of 3.6, 3.6, 3.6, 3.6, 4.0, and 4.0 nm[38]. These COFs with boronate ester linkage were applied in rapid photo-induced electron transfer and charge separation. In the same year, Xu *et al.* realized the synthesis of D_{TP}-A_{NDI}-COF with a pore size of 5.1 nm and coated it on carbon nanotubes as electrodes for battery devices[20]. In 2020, Zhao *et al.* reported ester-linked COF-122 with a pore size of 6.2 nm and a Brunauer-Emmett-Teller (BET) specific surface area of 908 m²/g, extending the 2D polyester family[24].
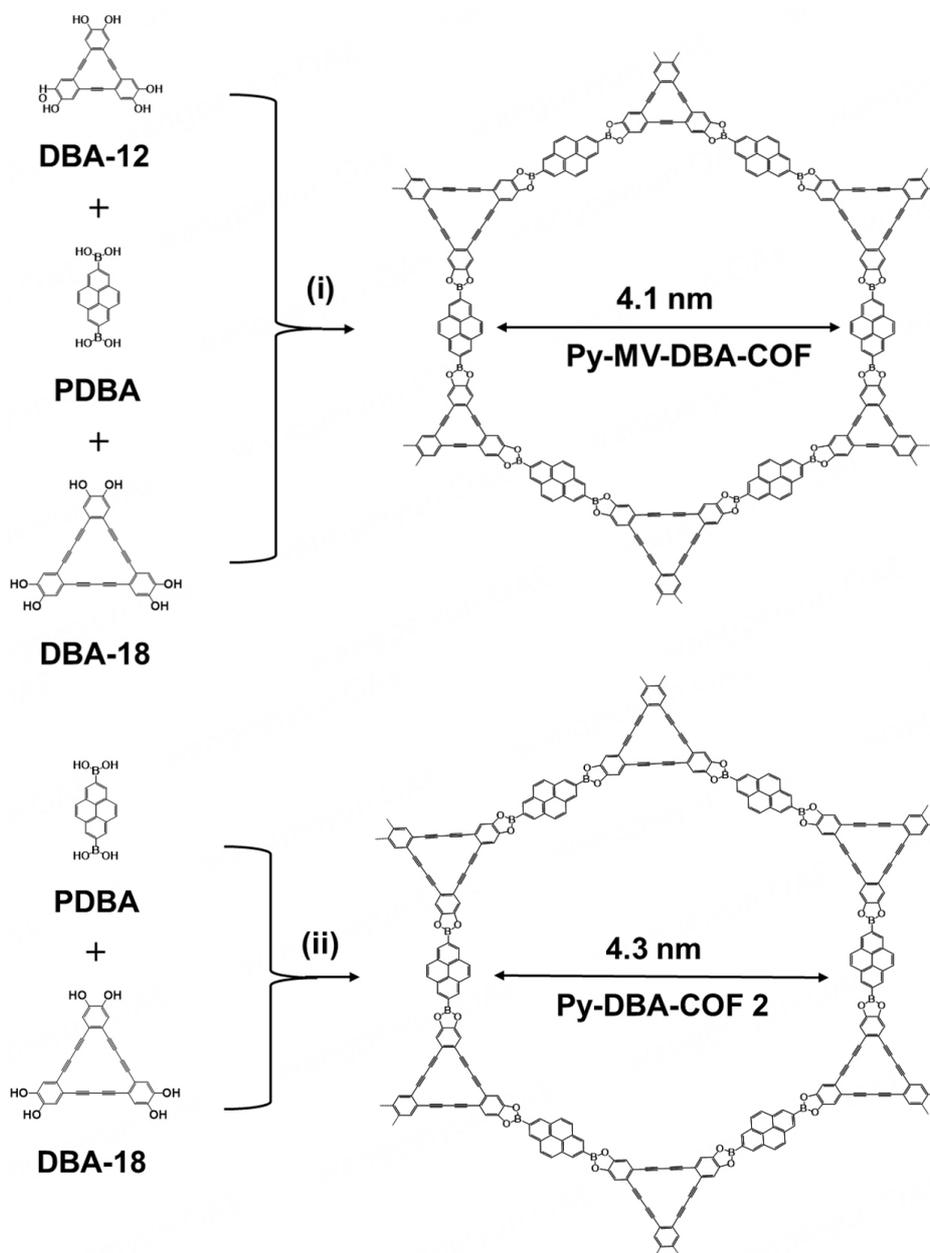
Figure 1. Schematics for the synthesis of Py-MV-DBA-COF and Py-DBA-COF 2. (i) 3-Pentanone/Mesitylene = 2/1 (*v/v*), 105 °C and 3 days; (ii) 3-Pentanone/Mesitylene = 2/1 (*v/v*), 105 °C and 3 days. DBA: Dehydrobenzoannulene; COF: covalent organic framework.

In 2014, Fang *et al.* successfully synthesized imide-linked COFs for the first time via the condensation reaction between extended aromatic dianhydrides and triamine building blocks[21]. Accordingly, a series of highly crystalline polyimide (PI)-COFs were yielded with a large pore size of 5.3 nm and a considerable surface area of 2,346 m²/g [Figure 2]. These PI-COFs are thermally robust up to 530 °C. Afterward, a large dye molecule, rhodamine B, with dimensions of about 10 × 16 Å², was incorporated into the pore of PI-COF-3 to make temperature-sensing devices, which is not possible for COFs with pore sizes less than 4.0 nm. Similar to PI-COFs, in 2020, Xu *et al.* reported that Ttba-TPDA-COF, with a pore size of 5.8 nm, exhibited superior dynamic adsorption capability for rhodamine B, highlighting its great potential in environmental remediation applications[23].
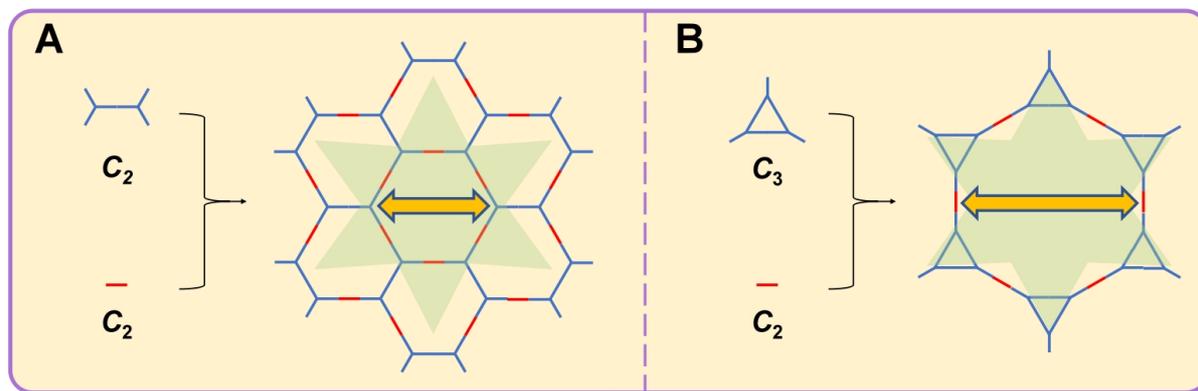
Scheme 1. Synthesis of 2D COFs with kgm topology via reactions of (A) C_2 and C_2-symmetric units and (B) C_3 and C_2-symmetric units. 2D: Two-dimensional; COFs: covalent organic frameworks.
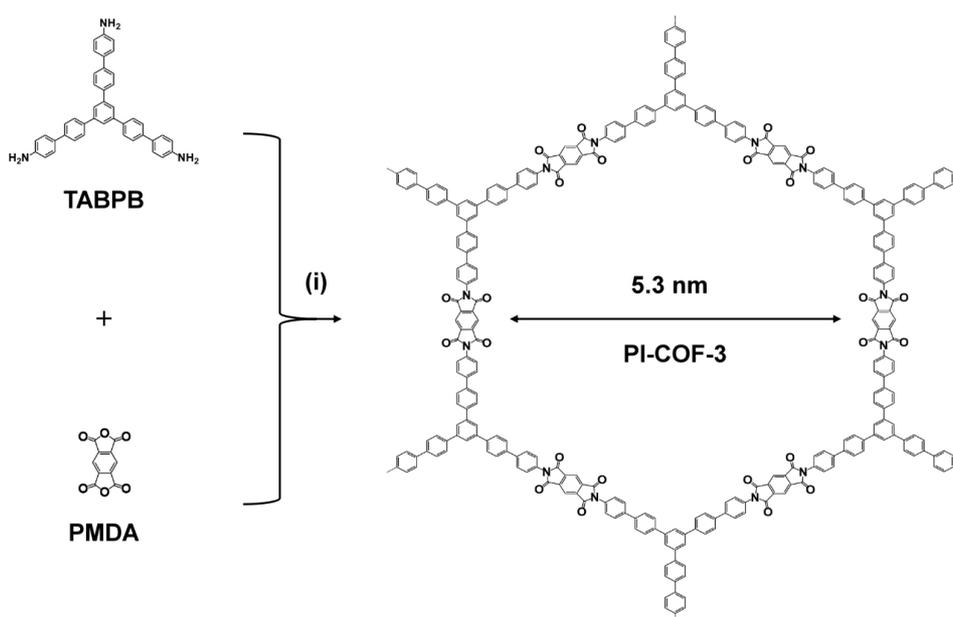

Figure 2. Skeleton design of PI-COF-3 with imide linkage. (i) Mesitylene/*N*-methyl-2-pyrrolidone/Isoquinoline = 1/1/1 (*v*/*v*/*v*), 250 °C and 7 days. COF: Covalent organic framework.

The most likely reason for the successful synthesis of large-pore boronate ester and imine-linked COFs is that the identical components of naphthalene diimide or perylene diimide contain fewer structural rotating sites than simple multi-phenyl ligands [Figure 3].

Fragment-oriented synthetic strategies

In 2016, Yu *et al.* reported an imine-linked polycationic (PC) 2D COF through the condensation of 1,3,5-tris(4-aminophenyl) benzene (TAPB) and 1,1-bis(4-formylphenyl)-4,4′-bipyridinium dichloride (BFBP^{2+}·2Cl$^-$)[22]. The resultant PC COF exhibits a hexagonal structure with a pore diameter of 5.8 nm [Figure 4]. The bipyridine (BIPY)-doped COF exhibits outstanding stability in water due to its PC nature and can almost quantitatively absorb anionic organic dyes in water at low concentrations. This makes the new PC COF a promising adsorbent for the removal of dye residues from water. The unique cationic BIPY-derived fragment with a large molecule size is believed to provide the structural basis for stabilizing the large
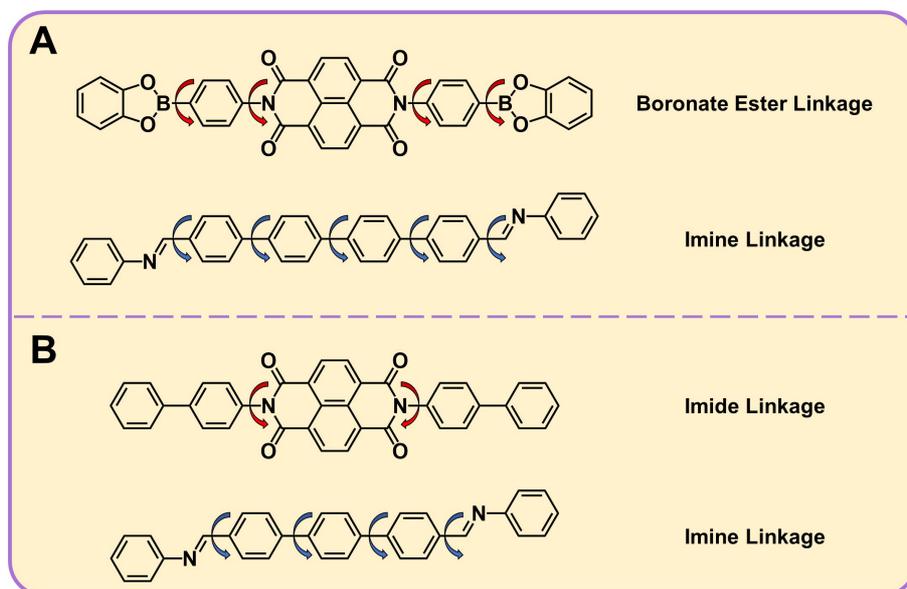
Figure 3. Comparison of naphthalene diimide units with (A) boronate ester linkage, (B) imide linkage, and imine-linked structures.
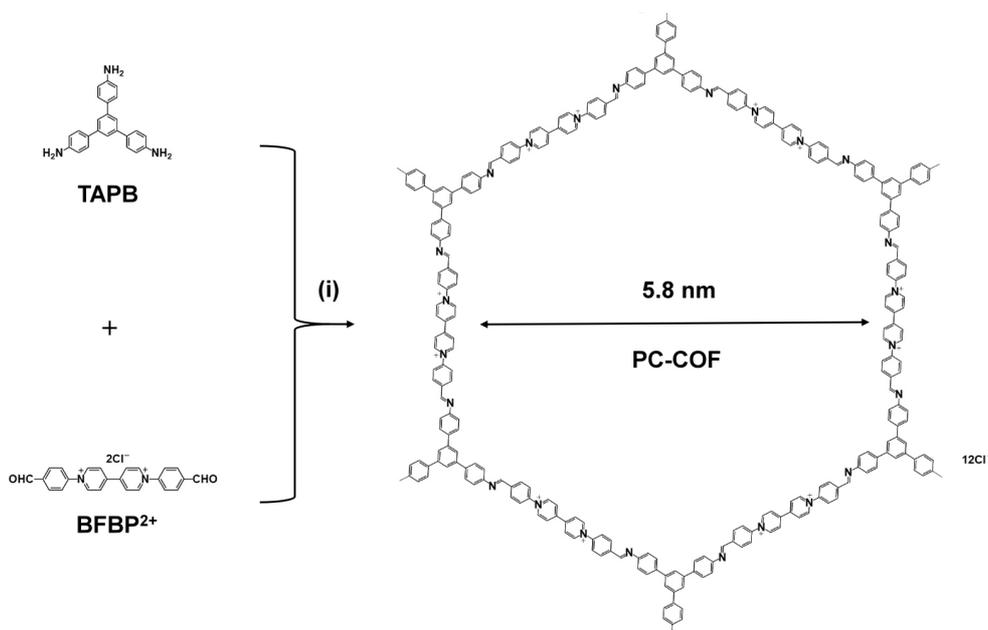

Figure 4. Synthesis route of PC-COF. (i) *o*-DCB:Ethanol = 9/1 (*v/v*), HAc (6 M), 120 °C and 7 days. TAPB: 1,3,5-tris(4-aminophenyl) benzene; BFBP^{2+}: 1,1-bis(4-formylphenyl)-4,4'-bipyridinium; COF: covalent organic framework; DCB: dichlorobenzene.

pore-sized 2D crystalline skeleton.

While the pore sizes of most reported MOFs are smaller than 3.0 nm[39], in 2015, Cho *et al.* reported a 4.9 nm-sized MOF with a strategy of incorporating pore-directing "anchors" (i.e., side chains) into building blocks to modulate the interlayer π-π interactions[40]. Along with this scenario, Emmerling *et al.* successfully obtained dpp-TAB COF and dpp-TAPB COF with pore sizes of 4.8 and 5.8 nm and surface areas of 1,467 m²/g and 1,670 m²/g, respectively [Figure 5][29]. The success lies in the use of methoxy groups as pore-
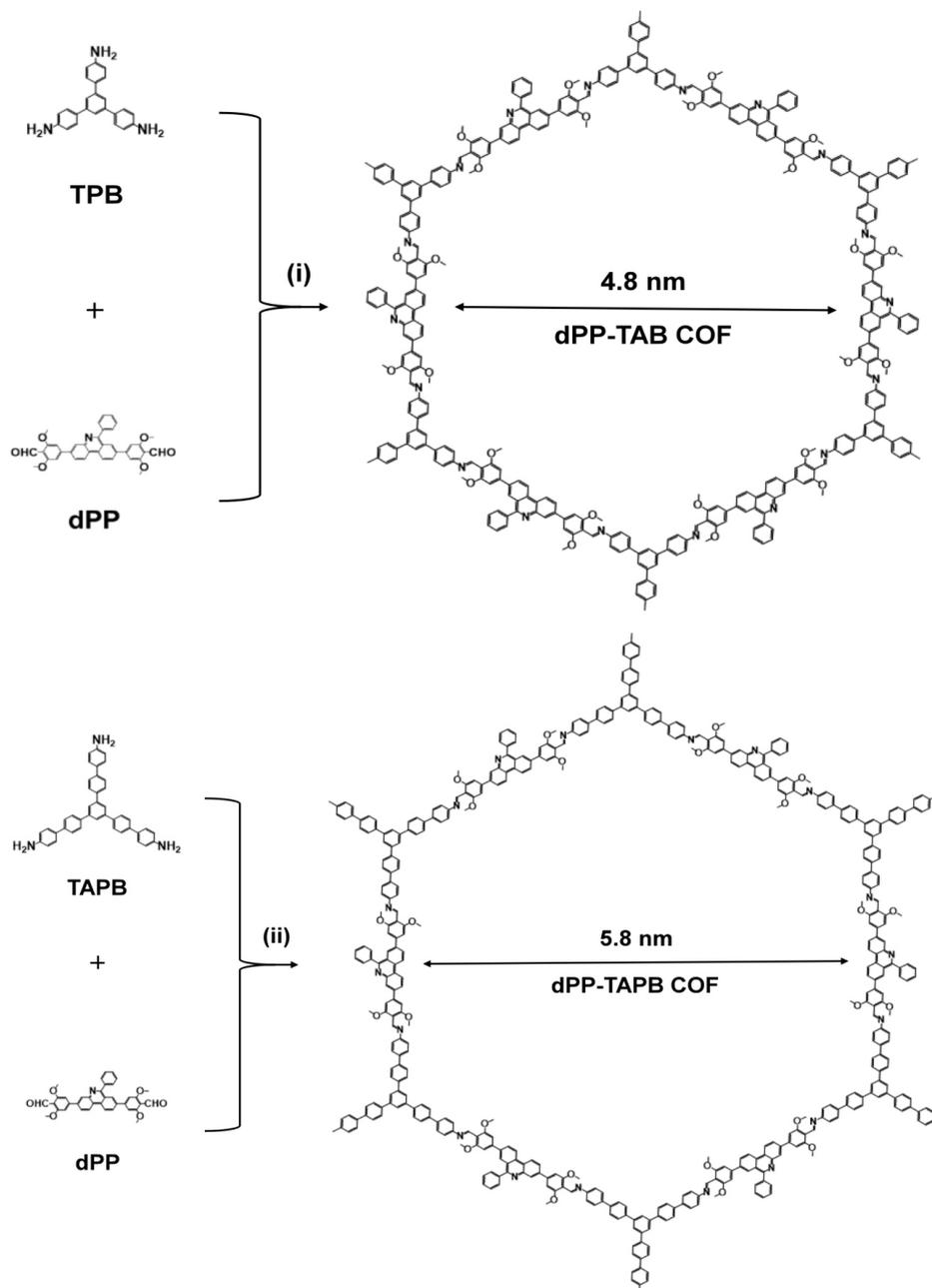
Figure 5. Synthesis routes of dPP-TAB COF and dPP-TAPB COF. (i) Mesitylene/1,4-Dioxane = 7/3 (*v/v*), HAc (12 M), 120 °C and 3 days; (ii) Mesitylene/1,4-Dioxane = 3/1 (*v/v*), HAc (6 M), 120 °C and 3 days. TAPB: 1,3,5-tris(4-aminophenyl) benzene; COF: covalent organic framework.

orientated "anchors" to prevent pore occlusion and collapse and ultimately produce highly crystalline and porous COFs.

As shown in Figure 6, the incorporation of methoxy substituents close to the imine linkage enables the diminishment of the intrinsic dipole moment and tuning of interlayer interactions. Consequently, the crystallinity of large porous lattices can be well maintained.
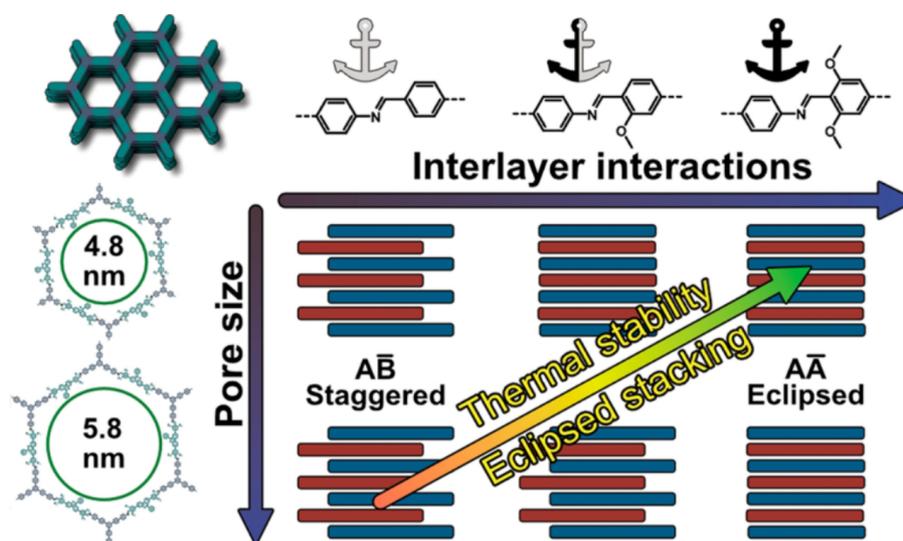
Figure 6. Schematic representation of the synthesis mechanism of large-pore dpp-TAPB COF. Reproduced with permission from ref.[29].Copyright © 2021 The Authors. Published by American Chemical Society. This publication is licensed under CC-BY 4.0. TAPB: 1,3,5-tris(4-aminophenyl) benzene; COF: covalent organic framework.

In 2022, based on the same strategy as above, Mu *et al.* realized the synthesis of a 2D COF with a record pore size of 10 nm, termed TDCOF-3 [Figure 7][41]. This milestone is achieved by creatively integrating methoxy side chains and alkyne units into a single monomeric structure. Such a combination not only enlarges the length of building blocks but also overcomes the intrinsic flexibility of growing polymeric chains. The resultant large pore-sized 2D COF is capable of separating 7.0 nm pepsin and protecting tyrosinase from heat-induced inactivation. Furthermore, this work also provides conclusive evidence that large mesoporous COFs can efficiently load enzymes of large molecular size and act as a protective layer to avoid enzyme inactivation under stringent conditions.

For TDCOF-3 with a pore size of 10.0 nm, the attachment of dimethoxy groups to the identical side of the phenyl ring also modulates interlayer interaction induced by local polarity. Besides, the insertion of carbon-carbon triple bonds to the main chain enhances the planarity and weakens the steric hindrance, leading to low nonbond energy. As a result, the ordered structure of TDCOF-3 with a record pore size was constructed with low nonbond energy [Figure 8].

For 3D COFs, the synthesis of large pore sizes is determined by various structural factors, and no definite mechanism has been reported in the literature. Therefore, the related explanations have been left for future work.

From the above examples, the approach of enlarging pore sizes of COFs by growing the length of monomer fragments is mainly available for hcb topological structures. For other topologies, the pore deformation might occur more significantly, making it more challenging to retain large pores.

As shown in Tables 1 and 2, the most common strategy for the synthesis of large pores is extending the length of the monomer fragments to increase the pore sizes of COFs, which ultimately leads to more intense pore collapses. To retain the large pore aperture, unique substituents, including methoxy, alkyl, *etc.*, have to be inserted into the building blocks, which increases the difficulty of monomer synthesis and leads to a sharp drop in total yield. Besides, researchers also choose to develop new topologies to create large pores,
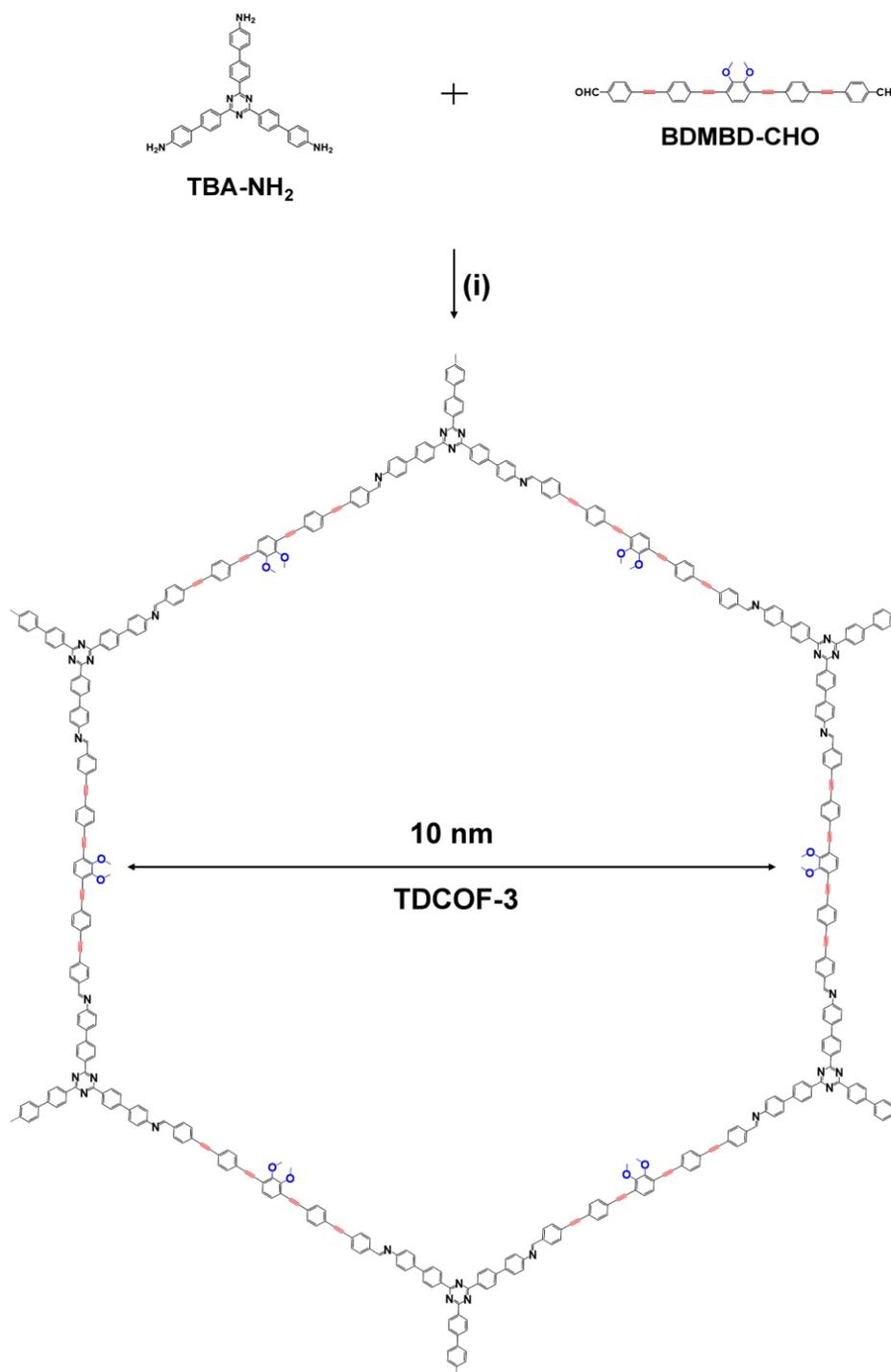
Figure 7. Schematic of TDCOF-3. (i) Mesitylene/1,4-Dioxane = 1/1 (*v/v*), HAc (6 M), 120 °C and 5 days.

which in itself is another challenge for COFs. From the above instances, reaction time plays a vital role in the synthesis of 2D large-pore COFs. The dynamic equilibrium of imine bond formation requires a longer time to form the large-pore COF with high crystallinity. Therefore, prolonging the time can be a potential approach to obtain large pores in 2D COFs.
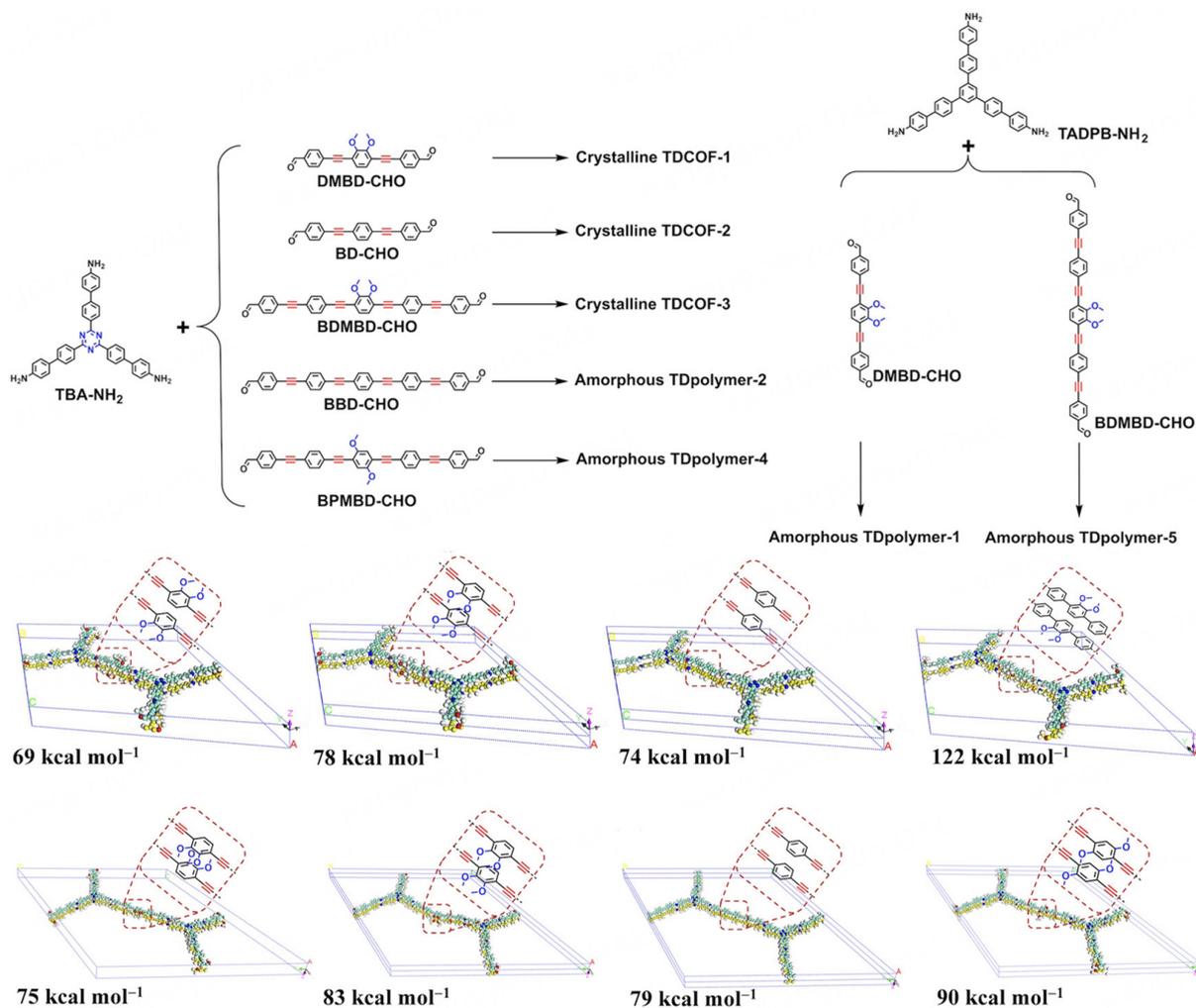
Figure 8. Calculation of the series of TDCOFs with the corresponding nonbond energies. Reproduced with permission from ref.[41]. Copyright © 2022, American Chemical Society.

OVERVIEW OF 3D COFS WITH LARGE PORES

Compared to 2D COFs with layered structures, the construction of 3D COFs with regular, periodic structures is proven to be a more complicated process. In particular, 3D COFs are generally less stable than 2D layered architectures due to more cavities and the lack of π-π stackings. Furthermore, 3D COFs tend to form cage-like structures when extended in three dimensions, and monomers can continue to react and grow outward in the cavity, which makes it easy for 3D COFs to generate multiple interspersed structures and more prone to collapse and shrinkage. Notably, the interpenetration between pores that occurs in diamondoid (dia) or pts topologies unfortunately leads to a high degree of channel constriction[42]. Taking these facts into account, current strategies for constructing 3D large-pore COFs mainly include (A) synthesizing monomers with side chains to prevent the collapse of large pores and (B) synthesizing novel topologies and fragments to construct large-pore size structures.

In sharp contrast to 2D COFs, the development history of large-pore 3D COFs is relatively new. In 2020, Wang *et al.* reported the work of expanding the pore size of 3D COFs up to 2.7 nm and achieving a high surface area of 3,023 m²/g through steric hindrance engineering[43]. It is worth noting that all JUC-550, 551,

Table 1. Summary of the porosity of the 2D COFs mentioned above

No.	Compound	Pore size (nm)[c]	BET (m²/g)	Major peak position (Degree)	Pore volume (cm³/g)	Ref.
1	D$_{CuPc}$-A$_{PDI}$-COF[b]	4.0	414	2.1	0.4	[38]
2	D$_{ZnPc}$-A$_{PDI}$-COF[b]	4.0	519	2.1	0.6	[38]
3	Py-MV-DBA-COF	4.1	1,134	2.3	1.1	[37]
4	Py-DBA-COF 2	4.3	1,354	2.2	1.2	[37]
5	Star-COF-2[b]	4.6	1,538	2.2	1.0	[35]
6	Star-COF-3[b]	4.7	1,489	2.2	1.1	[35]
7	PP-TAB[a,b]	4.8	1,063	1.5-2.0	1.1-1.5	[29]
8	mPP-TAB[a,b]	4.8	1,823	1.5-2.0	1.6-2.2	[29]
9	dPP-TAB[a]	4.8	1,467	1.5-2.0	-	[29]
10	D$_{TP}$-A$_{NDI}$-COF[a,b]	5.1	478	1.9	0.7	[20]
11	PI-COF-3	5.3	2,346	2.0	1.3	[21]
12	PC-COF	5.8	-	1.8	-	[22]
13	PP-TAPB[a]	5.8	1,032	1.2-1.8	3.1-3.3	[29]
14	mPP-TAPB[a]	5.8	631	1.2-1.8	0.6-0.8	[29]
15	dPP-TAPB[a]	5.8	1,670	1.2-1.8	-	[29]
16	Ttba-TPDA-COF	5.8	726	1.6	0.8	[23]
17	COF-122[a,b]	6.2	646	2.1	0.6	[24]
18	TDCOF-1	7.7	1,665	1.5	2.0	[41]
19	TDCOF-2	7.7	1,560	1.5	2.1	[41]
20	TDCOF-3	10	1,270	1.0	2.1	[41]

[a]Since the original articles did not mention the locations of the main peaks, we estimated them based on the PXRD patterns in the article. [b]The pore volumes of COFs were estimated based on the images in the articles. [c]Pore sizes are decided from the pore size distribution of the nitrogen sorption curves. 2D: Two-dimensional; COFs: covalent organic frameworks; DBA: dehydrobenzoannulene; TAPB: 1,3,5-tris(4-aminophenyl) benzene; PXRD: powder X-ray diffraction.

and 552 have non-interpenetrating dia topology by introducing methyl and methoxy groups into the building blocks [Figure 9]. For 3D COFs, it appears easier to shrink the pores or collapse the layers. As shown in Figure 10, either the (A) unmodified or (B) partially modified monomers result in shrinkage or interpenetration of the cavities[43]. Only the pores of the 3D COF built with (C) all modified units can be well maintained after the guest removal. Given that 3D cage-cavity organic structures are more prone to collapse, steric hindrance and expanding monomeric fragments are not feasible in producing large-pore 3D COFs, although they work well for creating large-pore 2D COFs.

Since the development of 3D COFs is relatively slow compared to 2D COFs and there are only two cases with pore sizes larger than 4.0 nm, we also include and discuss 3D COFs with pore sizes larger than 3.0 nm in this section.

Topology-oriented synthetic strategy
In 2007, the first 3D boronate ester-linked COF-108 was reported by El-Kaderi *et al.*, which exhibited boracite (bor) topology with a pore size of 3.0 nm[6]. In 2022, the first series of imine-linked COFs with bor topology were reported by Li *et al.*[44]. All three developed 3D-bor-COFs possess large pore sizes, i.e., 3.1 nm for 3D-bor-COF-1, 3.6 nm for 3D-bor-COF-2, and 3.8 nm for 3D-bor-COF-3 [Figure 11]. The obtained 3D COFs are excellent materials for capturing benzene vapor with adsorption capacities of 983.3 mg/g for 3D-bor-COF-1, 953.5 mg/g for 3D-bor-COF-2 and 1,203.9 mg/g for 3D-bor-COF-3.

Table 2. Summary of the synthetic strategies of 2D COFs

No.	Compound	Synthetic strategy	Ref.
1	Star-COF-2	Topology-oriented	[35]
2	Star-COF-3	Topology-oriented	[35]
3	Py-MV-DBA-COF	Topology-oriented	[37]
4	Py-DBA-COF 2	Topology-oriented	[37]
5	D_{CuPc}-A_{PDI}-COF	Linkage-oriented	[38]
6	D_{ZnPc}-A_{PDI}-COF	Linkage-oriented	[38]
7	D_{TP}-A_{NDI}-COF	Linkage-oriented	[20]
8	PI-COF-3	Linkage-oriented	[21]
9	Ttba-TPDA-COF	Linkage-oriented	[23]
10	COF-122	Linkage-oriented	[24]
11	PP-TAB	Fragment-oriented	[29]
12	mPP-TAB	Fragment-oriented	[29]
13	dPP-TAB	Fragment-oriented	[29]
14	PC-COF	Fragment-oriented	[22]
15	PP-TAPB	Fragment-oriented	[29]
16	mPP-TAPB	Fragment-oriented	[29]
17	dPP-TAPB	Fragment-oriented	[29]
18	TDCOF-1	Fragment-oriented	[41]
19	TDCOF-2	Fragment-oriented	[41]
20	TDCOF-3	Fragment-oriented	[41]

2D: Two-dimensional; COFs: covalent organic frameworks; DBA: dehydrobenzoannulene; TAPB: 1,3,5-tris(4-aminophenyl) benzene.

To date, only three COFs with bor topology have been reported, and all of them possess high specific surface areas and excellent crystallinity.

Fragment-oriented synthetic strategy

Recently, the exploration of specific fragments has also been considered a promising strategy for creating large-pore 3D COFs. For example, in 2020, Li *et al.* reported the synthesis of JUC-564 with an unprecedented stp topology, a pore size of 4.3 nm, and a large BET surface area of 3,383 m²/g [Figure 12][45]. The JUC-564 was synthesized through the condensation of specific 2,3,6,7,14,15-hexa(4′-formylphenyl) triptycene (HFPTP) with steric configuration and planar 1,3,6,8-tetrakis(4-aminophenyl) pyrene (TAPPy) units. By virtue of the large 3D porous channels, JUC-564 was utilized to load the biomolecule myoglobin with a molecular size of 21 Å × 35 Å × 44 Å.

On this basis, Ding *et al.* further reported another series of JUC-COFs using HFPTP as one of the monomers[46]. Notably, JUC-640-H achieved a record large pore size of 4.6 nm in 3D COFs with a surface area of 2,204 m²/g, which abundantly exposed porphyrin moieties (0.845 mmol/g) [Figure 13]. The JUC-640-Co containing the Co metalized porphyrin units was used for the photoreduction of CO_2 to CO, with a high CO generation rate of 15.1 mmol g/h and a selectivity of 94.4%. It is worth noting that the catalytic efficiency of JUC-640-Co exceeds all reported COF-based materials so far.

Since the development of 3D COFs is relatively new, synthetic strategies for 3D large-pore COFs rely on exploring novel topologies and specific fragments, as shown in Tables 3 and 4. However, both methods confront bottlenecks. For instance, it has been reported that only HFPTP can form large pores and react with other building blocks with distinct symmetries. The topologies of large pore apertures are limited to bor and stp, which requires further efforts to develop more topologies to build large pore-sized 3D COFs.
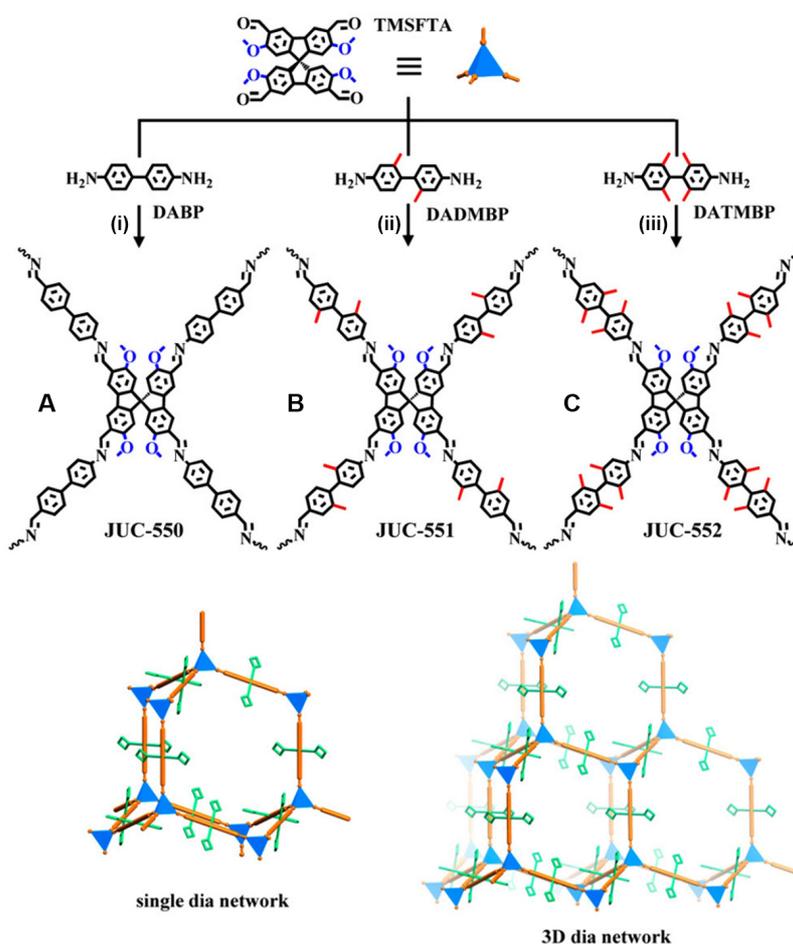
Figure 9. Synthesis routes of (A) JUC-550; (B) JUC-551; and (C) JUC-552. (i) 1,4-Dioxane, 120 °C and 3 days; (ii) Mesitylene, 120 °C and 3 days; (iii) Mesitylene, 120 °C and 3 days. Reproduced with permission from ref.[43]. Copyright © 2020, American Chemical Society. 3D: Three-dimensional.

Notably, because cage cavity structures are more prone to shrinkage, most works adopted immersion powder for activation, and some of them even utilized supercritical carbon dioxide during the post-treatment of COFs.

CONCLUSION AND OUTLOOK

Similar to other porous materials, the structural characteristics and application performance of COFs are highly dependent on their porosity, especially pore size. In particular, COFs with large mesopores enable the entry of unique large-sized guest molecules, which undoubtedly expands their functionalities. Therefore, it is crucial to develop efficient approaches to design and synthesize large pore-sized COFs rationally. In this work, we review several state-of-the-art strategies for producing large-pore COFs shown in Tables 2 and 4, including (A) designing COFs with specific topologies, such as hcb, kgm, stp, bor, *etc.*; (B) using imide linkage to prepare target COFs; (C) employing sizeable molecular building blocks with charged part or side chains to prevent shrinkage of large-pore and interlayer slippage; and (D) developing organic unit with unique steric configurations to maintain large pores in 3D COFs. We call upon the fact that despite significant progress in this appealing research area, the synthetic mechanisms remain elusive. Further efforts combining molecular-level simulations and in situ structural characterization may provide a microscopic view of the large-pore formation.
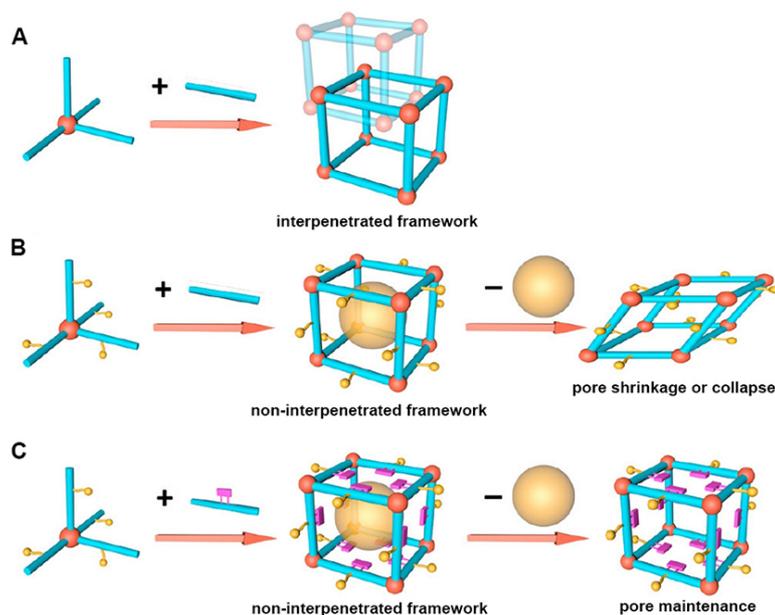
Figure 10. Synthesis for 3D mesoporous COFs for three possible: (A) unmodified; (B) partially modified units; and (C) all modified units. Reproduced with permission from ref.[43]. Copyright © 2020, American Chemical Society. 3D: Three-dimensional; COFs: covalent organic frameworks.
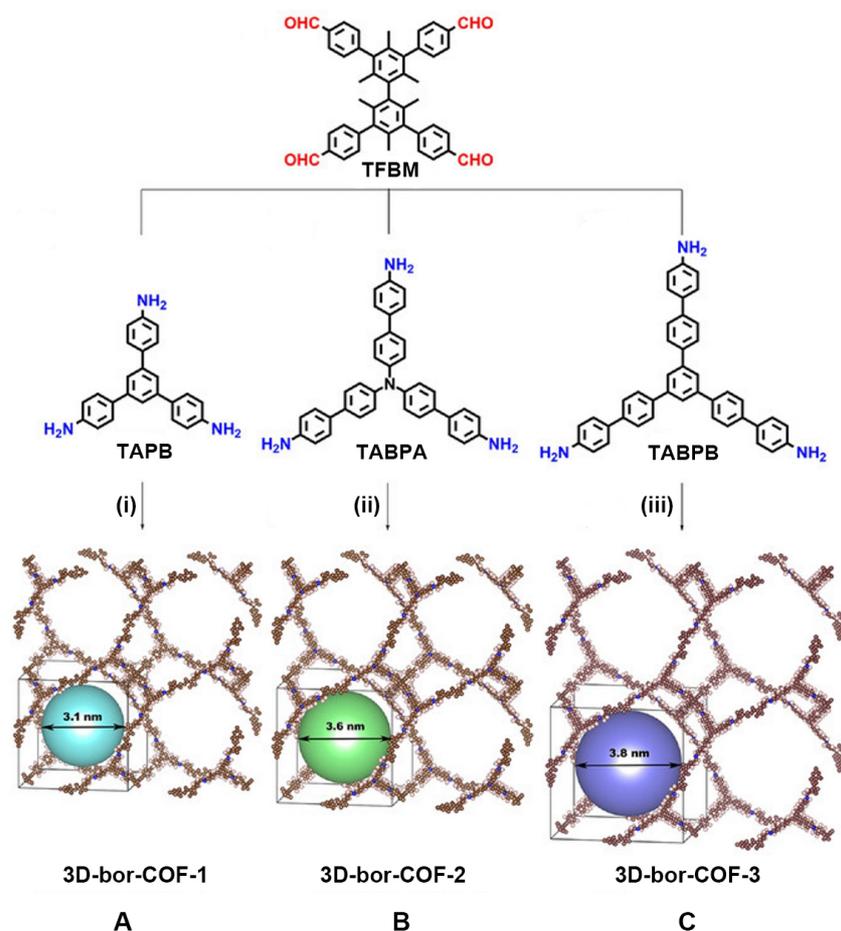

Figure 11. Synthesis routes of (A) 3D-bor-COF 1; (B) 3D-bor-COF 2; (C) 3D-bor-COF 3; (i) *o*-DCB, HAc (6 M), 120 °C and 4 days; (ii) *o*-DCB, HAc (6 M), 120 °C and 4 days; (iii) *o*-DCB, HAc (6 M), 120 °C and 4 days. Reproduced with permission from ref.[44]. Copyright © 2022 The Authors. SusMat published by Sichuan University and John Wiley & Sons Australia, Ltd. TAPB: 1,3,5-tris(4-aminophenyl) benzene; 3D: three-dimensional; COF: covalent organic framework; DCB: dichlorobenzene.
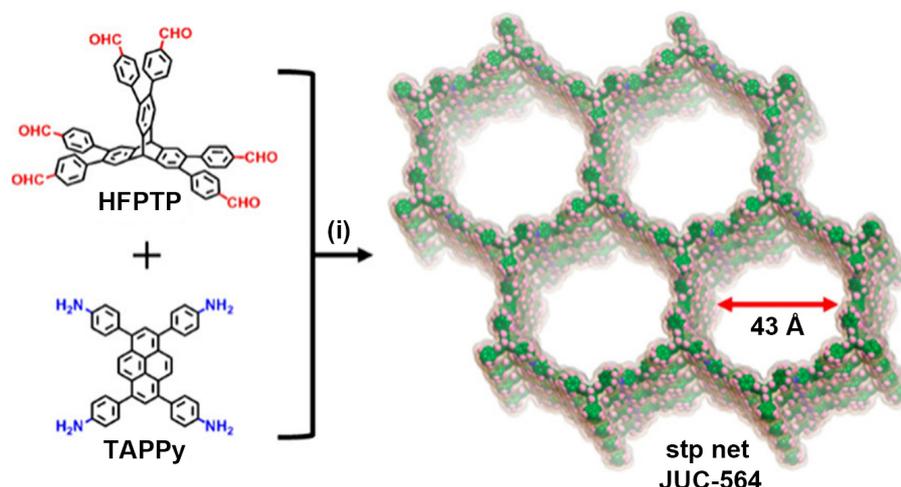
Figure 12. Synthesis route of JUC-564. (i) Mesitylene/1,4-Dioxane = 3/2 (*v/v*), HAc (6 M), 120 °C and 3 days. Reproduced with permission from ref.[45]. Copyright © 2020, American Chemical Society. HFPTP: 2,3,6,7,14,15-hexa(4'-formylphenyl)triptycene; TAPPy: 1,3,6,8-tetrakis(4-aminophenyl) pyrene.
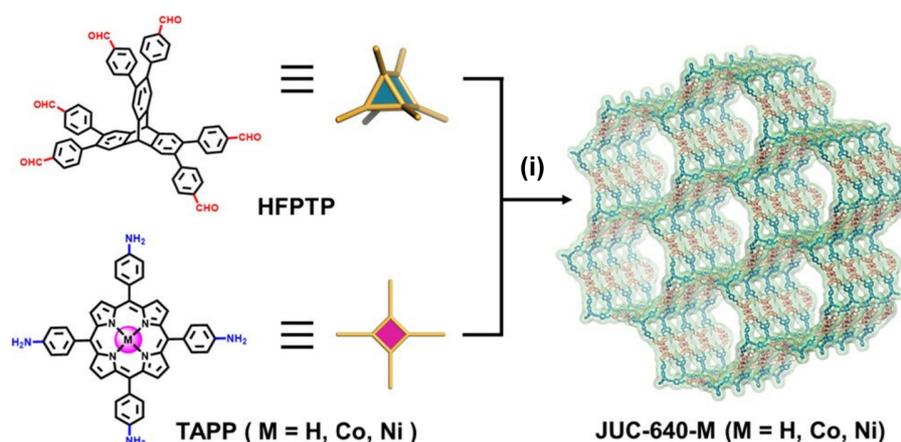

Figure 13. Synthesis scheme of JUC-640-M. (i) *o*-DCB/*n*-BuOH = 1/1, HAc (6 M), 120 °C and 7 days. Reproduced with permission from ref.[46]. Copyright © 2023, American Chemical Society. HFPTP: 2,3,6,7,14,15-hexa(4'-formylphenyl)triptycene; DCB: dichlorobenzene.

As discussed above, most reported preparations of large pore-sized COFs still rely on simply increasing the length of the building blocks, but this results in low overall reaction yields and a tendency for structural collapse or interlayer interpenetration. Although several fragments with specific steric configurations can yield large pore-sized 3D COFs, the intrinsic relationship between structure and pore size is still unclear. In addition, all COFs with large pores reported to date are prepared using organic units with imine or boronic ester linkages, which also limits stability and subsequent functional exploration. Developing large-pore COFs with other linkages remains a challenge and requires further efforts.

Regardless of 2D COFs or 3D COFs, the pore collapse and blockage of the frameworks due to the extended length and high flexibility cannot be evaded. Therefore, an effective way needs to be proposed to retain the large porous networks. For instance, multi-bond linked COFs can be designed with relatively small pores and robust skeletons. The large-pore COFs can be generated by dissociating one or partial bonds under reverse conditions. Besides, there is an urgent need to explore a facile substituent that can

Table 3. Summary of the porosity of the 3D COFs mentioned above

No.	Compound	Pore size (nm)[b]	BET (m^2/g)	Major peak position (Degree)	Ref.
1	JUC-552	2.65	3,023	3.3	[43]
2	3D-bor-COF-1	3.1	983.3	2.1	[44]
3	3D-bor-COF-2	3.6	953.5	2.0	[44]
4	3D-bor-COF-3	3.8	1,203.9	1.7	[44]
5	JUC-564	4.3	3,383	1.9	[45]
6	JUC-640-H[a]	4.6	2,204	1.1-1.5	[46]

[a]Since the original article did not mention the location of the main peaks of COFs, we roughly estimated them based on the PXRD given in the article. [b]Pore sizes are decided from the pore size distribution of the nitrogen sorption curves. 3D: Three-dimensional; COFs: covalent organic frameworks; BET: Brunauer-Emmett-Teller; PXRD: powder X-ray diffraction.

Table 4. Summary of the synthetic strategies of 3D COFs

No.	Compound	Synthetic strategy	Ref.
1	JUC-552	Steric hindrance-oriented	[43]
2	3D-bor-COF-1	Topology-oriented	[44]
3	3D-bor-COF-2	Topology-oriented	[44]
4	3D-bor-COF-3	Topology-oriented	[44]
5	JUC-564	Fragment-oriented	[45]
6	JUC-640-H	Fragment-oriented	[46]

3D: Three-dimensional; COFs: covalent organic frameworks.

effectively control the interlayer slip of 2D COFs to maintain large pores. As mentioned above, either AB or ABC stacking will lead to a reduction in pore size. Thus, it is crucial to synthesize available groups to construct building blocks that ensure AA stacking. Lastly, a potential template-assisted strategy can be proposed and used to support pores from collapse during post-treatment. Afterward, the templates were completely removed under mild conditions.

We emphasize that an ideal and effective strategy for designing large pore-sized COFs should not only produce regular porous structures with good structural stability but also have simple synthetic processes, high total reaction yields, and great generality. Such an efficient synthetic approach needs to be proposed and developed in the future. It is hoped that the continuous development of large mesoporous COFs will extend and promote their applications in more specific fields, including but not limited to the absorption and separation of macromolecules, bio-catalysis, *etc.*

DECLARATIONS

Authors' contributions
Prepared and revised the manuscript: Li X
Revised the manuscript: Geng K, Fu S
Designed and revised the manuscript: Jin E
All authors contributed to the discussion and preparation of the manuscript.

Conflicts of interest
All authors declared that there are no conflicts of interest.

Ethical approval and consent to participate
Not applicable.

Consent for publication
Not applicable.

REFERENCES

1. Alsbaiee A, Smith BJ, Xiao L, Ling Y, Helbling DE, Dichtel WR. Rapid removal of organic micropollutants from water by a porous β-cyclodextrin polymer. *Nature* 2016;529:190-4. DOI PubMed
2. Zheng B, Lin X, Zhang X, Wu D, Matyjaszewski K. Emerging functional porous polymeric and carbonaceous materials for environmental treatment and energy storage. *Adv Funct Mater* 2020;30:1907006. DOI
3. Huang L, Yang J, Zhao Y, et al. Monolithic covalent organic frameworks with hierarchical architecture: attractive platform for contaminant remediation. *Chem Mater* 2023;35:2661-82. DOI
4. Yuan Y, Yang Y, Meihaus KR, et al. Selective scandium ion capture through coordination templating in a covalent organic framework. *Nat Chem* 2023;15:1599-606. DOI
5. Côté AP, Benin AI, Ockwig NW, O'Keeffe M, Matzger AJ, Yaghi OM. Porous, crystalline, covalent organic frameworks. *Science* 2005;310:1166-70. DOI PubMed
6. El-Kaderi HM, Hunt JR, Mendoza-Cortés JL, et al. Designed synthesis of 3D covalent organic frameworks. *Science* 2007;316:268-72. DOI
7. Zhuang X, Zhao W, Zhang F, et al. A two-dimensional conjugated polymer framework with fully sp^2-bonded carbon skeleton. *Polym Chem* 2016;7:4176-81. DOI
8. Jin E, Asada M, Xu Q, et al. Two-dimensional sp^2 carbon-conjugated covalent organic frameworks. *Science* 2017;357:673-6. DOI
9. Ma T, Kapustin EA, Yin SX, et al. Single-crystal x-ray diffraction structures of covalent organic frameworks. *Science* 2018;361:48-52. DOI
10. Feng X, Ding X, Jiang D. Covalent organic frameworks. *Chem Soc Rev* 2012;41:6010-22. DOI PubMed
11. Ding SY, Wang W. Covalent organic frameworks (COFs): from design to applications. *Chem Soc Rev* 2013;42:548-68. DOI PubMed
12. Sun C, Sheng D, Wang B, Feng X. Covalent organic frameworks for extracting water from air. *Angew Chem Int Ed Engl* 2023;62:e202303378. DOI
13. Burke DW, Jiang Z, Livingston AG, Dichtel WR. 2D covalent organic framework membranes for liquid-phase molecular separations: state of the field, common pitfalls, and future opportunities. *Adv Mater* 2024;36:e2300525. DOI PubMed
14. Liang RR, Jiang SY, A RH, Zhao X. Two-dimensional covalent organic frameworks with hierarchical porosity. *Chem Soc Rev* 2020;49:3920-51. DOI PubMed
15. Huang N, Wang P, Jiang D. Covalent organic frameworks: a materials platform for structural and functional designs. *Nat Rev Mater* 2016;1:16068. DOI
16. Diercks CS, Yaghi OM. The atom, the molecule, and the covalent organic framework. *Science* 2017;355:eaal1585. DOI PubMed
17. Chen X, Geng K, Liu R, et al. Covalent organic frameworks: chemical approaches to designer structures and built-in functions. *Angew Chem Int Ed Engl* 2020;59:5050-91. DOI
18. Kandambeth S, Dey K, Banerjee R. Covalent organic frameworks: chemistry beyond the structure. *J Am Chem Soc* 2019;141:1807-22. DOI PubMed
19. Jin S, Furukawa K, Addicoat M, et al. Large pore donor-acceptor covalent organic frameworks. *Chem Sci* 2013;4:4505-11. DOI
20. Xu F, Jin S, Zhong H, et al. Electrochemically active, crystalline, mesoporous covalent organic frameworks on carbon nanotubes for synergistic lithium-ion battery energy storage. *Sci Rep* 2015;5:8225. DOI PubMed PMC

21. Fang Q, Zhuang Z, Gu S, et al. Designed synthesis of large-pore crystalline polyimide covalent organic frameworks. *Nat Commun* 2014;5:4503. DOI

22. Yu SB, Lyu H, Tian J, et al. A polycationic covalent organic framework: a robust adsorbent for anionic dye pollutants. *Polym Chem* 2016;7:3392-7. DOI

23. Xu T, An S, Peng C, Hu J, Liu H. Construction of large-pore crystalline covalent organic framework as high-performance adsorbent for rhodamine B dye removal. *Ind Eng Chem Res* 2020;59:8315-22. DOI

24. Zhao C, Lyu H, Ji Z, Zhu C, Yaghi OM. Ester-linked crystalline covalent organic frameworks. *J Am Chem Soc* 2020;142:14450-4. DOI

25. Vyas VS, Vishwakarma M, Moudrakovski I, et al. Exploiting noncovalent interactions in an imine-based covalent organic framework for quercetin delivery. *Adv Mater* 2016;28:8749-54. DOI

26. Liu S, Hu C, Liu Y, Zhao X, Pang M, Lin J. One-pot synthesis of DOX@covalent organic framework with enhanced chemotherapeutic efficacy. *Chemistry* 2019;25:4315-9. DOI

27. Zhang G, Li X, Liao Q, et al. Water-dispersible PEG-curcumin/amine-functionalized covalent organic framework nanocomposites as smart carriers for in vivo drug delivery. *Nat Commun* 2018;9:2785. DOI PubMed PMC

28. Zhao X, Pachfule P, Li S, et al. Macro/microporous covalent organic frameworks for efficient electrocatalysis. *J Am Chem Soc* 2019;141:6623-30. DOI

29. Emmerling ST, Schuldt R, Bette S, et al. Interlayer interactions as design tool for large-pore COFs. *J Am Chem Soc* 2021;143:15711-22. DOI PubMed PMC

30. Qian C, Wu H, Teo WL, Liao Y, Zhao Y. Single-crystalline covalent organic frameworks. *Trends Chem* 2023;5:853-67. DOI

31. Huang L, Yang J, Asakura Y, Shuai Q, Yamauchi Y. Nanoarchitectonics of hollow covalent organic frameworks: synthesis and applications. *ACS Nano* 2023;17:8918-34. DOI

32. Qian C, Teo WL, Gao Q, Wu H, Liao Y, Zhao Y. Polycrystalline covalent organic frameworks. *Mater Today* 2023;71:91-107. DOI

33. Lukose B, Kuc A, Frenzel J, Heine T. On the reticular construction concept of covalent organic frameworks. *Beilstein J Nanotechnol* 2010;1:60-70. DOI PubMed PMC

34. Lukose B, Kuc A, Heine T. The structure of layered covalent-organic frameworks. *Chemistry* 2011;17:2388-92. DOI PubMed

35. Feng X, Dong Y, Jiang D. Star-shaped two-dimensional covalent organic frameworks. *CrystEngComm* 2013;15:1508-11. DOI

36. Zhou TY, Xu SQ, Wen Q, Pang ZF, Zhao X. One-step construction of two different kinds of pores in a 2D covalent organic framework. *J Am Chem Soc* 2014;136:15885-8. DOI

37. Crowe JW, Baldwin LA, McGrier PL. Luminescent covalent organic frameworks containing a homogeneous and heterogeneous distribution of dehydrobenzoannulene vertex units. *J Am Chem Soc* 2016;138:10120-3. DOI PubMed

38. Jin S, Supur M, Addicoat M, et al. Creation of superheterojunction polymers via direct polycondensation: segregated and bicontinuous donor-acceptor π-columnar arrays in covalent organic frameworks for long-lived charge separation. *J Am Chem Soc* 2015;137:7817-27. DOI

39. Su Y, Yuan G, Hu J, et al. Recent progress in strategies for preparation of metal-organic frameworks and their hybrids with different dimensions. *Chem Synth* 2023;3:1. DOI

40. Cho HS, Deng H, Miyasaka K, et al. Extra adsorption and adsorbate superlattice formation in metal-organic frameworks. *Nature* 2015;527:503-7. DOI

41. Mu Z, Zhu Y, Li B, Dong A, Wang B, Feng X. Covalent organic frameworks with record pore apertures. *J Am Chem Soc* 2022;144:5145-54. DOI

42. Guan X, Chen F, Fang Q, Qiu S. Design and applications of three dimensional covalent organic frameworks. *Chem Soc Rev* 2020;49:1357-84. DOI

43. Wang Y, Liu Y, Li H, et al. Three-dimensional mesoporous covalent organic frameworks through steric hindrance engineering. *J Am Chem Soc* 2020;142:3736-41. DOI

44. Li Z, Hsueh C, Tang Z, et al. Rational design of imine-linked three-dimensional mesoporous covalent organic frameworks with bor topology. *SusMat* 2022;2:197-205. DOI

45. Li H, Ding J, Guan X, et al. Three-dimensional large-pore covalent organic framework with stp topology. *J Am Chem Soc* 2020;142:13334-8. DOI

46. Ding J, Guan X, Lv J, et al. Three-dimensional covalent organic frameworks with ultra-large pores for highly efficient photocatalysis. *J Am Chem Soc* 2023;145:3248-54. DOI